Supporting Information

Callura et al. 10.1073/pnas.1009747107

SI Text

GFP-TonB Images. Additional examples of representative micrographs from each GFP-TonB experimental setup and condition are presented in Fig. S1.

Phenotypic Analyses of CcdB Expression. Before starting any in vivo analysis of the CcdB toxin, riboregulation was necessary to successfully transform a plasmid containing the *ccdB* gene. In our study, viable MG1655 colonies were visible only following transformation with our uninduced CcdB riboregulator [RR12(14) CcdB]; induction of CcdB translation significantly reduced colony number (Fig. S2*A*). Viable colonies were not obtained following transformation of our control plasmid [pL(tetO)-CcdB], which lacks the *cis*-repressive sequence (Fig. S2*A*).

In addition to the transcriptome analysis presented in Fig. 3*B*, we also performed experiments that explored the phenotypic response of MG1655 and MG1063 cells to riboregulated CcdB expression to demonstrate the potency of the toxin. Initially, we measured optical density (OD_{600}) at 600 nm. In both strains, the growth rate was arrested prematurely upon induction of CcdB translation (Fig. S2 *B* and *C*). By comparison, we observed no noticeable changes in growth for uninduced cultures (harboring the CcdB riboregulator system) or for induced cultures containing a LacZ riboregulator control (constructed by replacing the *ccdB* gene with the *lacZ* gene encoding galactosidase) (Fig. S2 *B* and *C*).

To determine the level of cell killing achievable using the CcdB riboregulator, we performed viable cell counts on samples taken immediately before and after different levels of CcdB induction. Full activation of CcdB expression in MG1655 cells resulted in a dramatic 3-log decrease in survival within the first 30 min postinduction (Fig. S2*D*); survival declined nearly 4.5-log over the duration of the experiment. In MG1063 cells, full activation of CcdB expression reproducibly resulted in an immediate 2.5-log decrease and a marked 5-log decrease (approaching our limit of detection) in survival by 2.5 h postinduction (Fig. S2*E*). Low and intermediate induction of CcdB expression expectedly resulted in a graded response to gyrase inhibition in both strains (>2- and >3-log decreases in survival, respectively, at 2.5 h postinduction) (Fig. S2 *D* and *E*).

These data suggest that DNA is damaged and cells are overwhelmed soon after build-up of excess CcdB occurs. This hypothesis was supported by micrographs of fully induced cultures (Fig. S3). From these images, it is clear that CcdB expression rapidly (≤30 min postinduction) results in cell filamentation and arrest of cell growth. This finding confirms the previous hypothesis that filamentation is related to the mechanism of cell killing (1). Additionally, these images clearly show that CcdB expression can induce SOS-independent filamentation, consistent with previous work (2).

Taken together, our results showcase the potent toxicity of the CcdB toxin and the increased susceptibility of MG1063 cells to CcdB expression. With respect to the features of the riboregulator system, graded levels of survival (Fig. S2 *D* and *E*) illustrate gene expression tunability. Perhaps more importantly, these results demonstrate the utility of the riboregulator system in approximating the postsegregational killing effect of CcdB, because the timing of the observed phenotypic responses is more in line with the timing of Lon-mediated proteolysis of antitoxins than previous studies involving temperature-sensitive replication arrest (3, 4).

Raw Relative mRNA Concentrations. To demonstrate the riboregulator system's tunability, we treated cells with DNA-damaging norfloxacin and expressed different levels of LexA3. We determined the graded response to this treatment, in part, by measuring the fold changes in relative mRNA concentrations for *recA*, *recN*, *sulA*, and *umuC* (Fig. 3*C*). As referenced in the main text, the raw relative mRNA concentrations for the selected SOS genes are presented in Fig. S4. These values are not normalized by the corresponding untreated relative mRNA concentrations and thus depict the differences in mRNA abundance between the SOS genes.

Glucose Requirement in Orthogonal Riboregulation Experiments. As observed in Fig. 5, the *λR-R*$_Z$ and *λS* genes were independently regulated by two riboregulator variants. Initial experiments independently expressing λS only without glucose resulted in a strong degree of cell lysis (Fig. S5). In this case, both λS and λR-R_Z mRNA [regulated by anhydrotetracycline (aTc)-inducible $P_{LtetO-1}$] are fully induced and present at high concentrations (Fig. 5*A*). The λS taRNA (regulated by IPTG-inducible $P_{LlacO-1}$) also is fully induced, activating translation of λS. The amount of λR-R_Z translation is dependent solely on the leakage from arabinose-inducible P_{BAD}. In addition, it is important to note that the riboregulator variant (crR10-taR10) containing *λR-R*$_Z$ has been shown to have a slightly higher basal expression level than the variant (crR12-taR12) containing *λS* (5).

To reduce the amount of λR-R_Z leakage, we added 0.2% glucose, which lowers expression from P_{BAD} through catabolite repression (6). The addition of glucose abolished lysis (Fig. 5*B*). In addition, we tested three more conditions: +1 mM IPTG + 0.01% arabinose (no λS or λR-R_Z crRNA), +30 ng/mL aTc only (no λS or λR-R_Z taRNA), and full induction (+30 ng/mL aTc + 1 mM IPTG) of a strain that contained only the λS riboregulator. In each of these samples, no lysis was observed (Fig. S5). Therefore, the following conclusions about our orthogonal riboregulation setup can be made: When λS crRNA and taRNA and λR-R_Z crRNA are fully induced, further repression of P_{BAD} with glucose prevents lysis; when either λS crRNA or taRNA remains uninduced, the minimal amount of λR-R_Z leakage cannot lyse cells; and λS cannot lyse cells alone, confirming previous work (7).

These additional experiments suggest that the sensitivity of the cell to λR-R_Z levels was mainly responsible for the OD_{600} drop observed in the high λS induction only–no glucose culture (Fig. S5). Our CcdB results showed that the *cis*-repression of a fully induced crRNA results in a minimal amount of expression when the taRNA is regulated by P_{BAD} (Figs. S2 and S3). The same regulation setup occurs for λR-R_Z in the high λS induction only–no glucose case; however, in the orthogonal riboregulation setup, the cell is very sensitive to the effects of λR-R_Z. We showed in Fig. 5*E* and Fig. S6 that low and high λR-R_Z expression levels have approximately the same effect at various λS concentrations; more specifically, high λS expression resulted in widespread cell lysis at low λR-R_Z concentrations. Despite the λR-R_Z taRNA remaining uninduced, leakage from P_{BAD} plus the increased basal expression from the crR10-taR10 riboregulator variant resulted in an expression level that was large enough to cause lysis in the highly sensitive, high λS induction only–no glucose culture. The requirement for glucose to prevent lysis in this case has no bearing on the other orthogonal riboregulation experiments. Independent regulation of the λ-phage lysis proteins was achieved, regardless of the slightly increased basal expression of λR-R_Z. This unexpected result emphasizes the need for tighter inducible promoters.

Methods. ***Strains.*** For experimental purposes, we used four related *E. coli* K-12 derivative strains, MG1655 (F−, λ−; ATCC no.

47076) (8), MG1063 (F+, λ–, *recA56*, *thi*; Yale CGSC no. 6199) (9), MG1655Pro (F–, λ–, Sp^r, *lacR*, *tetR*) (10), and MG1655ProΔ*tonB*. For cloning purposes, we used the XL-10 strain [Stratagene; *Tet*(*mcrA*)183, (*mcrCB-hsdSMR-mrr*)173, *endA1*, *supE44*, *thi-1*, *recA1*, *gyrA96*, *relA1*, *lac Hte* [F *proAB* $lacI^q$ *Z*Δ*M15* Tn10 (Tet^r) *Amy* Cam^r]] in constructing the CcdB riboregulator system and MG1655Pro in constructing all other plasmids. To make the MG1655ProΔ*tonB* strain, we first used P1 transduction to transfer the *tonB*::*kanR* cassette from the Keio *E. coli* single-gene knockout library to MG1655 (11). The *kanR* gene was subsequently excised using the PCP20 λ-recombinase system (12). Finally, we again used P1 transduction to transfer the Pro cassette from MG1655Pro to MG1655Δ*tonB* (10).

Plasmid construction. All plasmids were built using restriction endonucleases and T4 DNA Ligase from New England Biolabs (NEB) and verified by restriction analysis. Riboregulation systems were based on our published design (13). Plasmids were transformed using standard heat-shock protocols (14). All cells were grown in selective medium: Luria–Bertani (LB) media (Fisher) supplemented with 30 μg/mL of kanamycin (Fisher). Plasmid isolation was performed using QIAprep Spin Miniprep kits (Qiagen). Table S1 contains an overview of all plasmids constructed.

For the protein tracking experiments, we cloned the genes encoding GFP and TonB (separated by a short linker sequence and based on a previous design) (15) into the riboregulator system in two steps. First, we constructed a PCR fragment consisting of the linker and the *tonB* gene. Sequential PCR steps added the codons encoding the helical linker (AEAAAKA) (16) to the N-terminal sequence of *tonB* after the initial methionine codon. Also, we added KpnI and NheI restriction endonuclease recognition sites to the N-terminal sequence of the fragment and a HindIII recognition site to the C-terminal sequence. The first cloning step used the restriction endonucleases KpnI and HindIII (NEB) to insert this PCR fragment into the riboregulator system. Next, we inserted the gfp^+ gene (17) with the restriction endonucleases KpnI and NheI (NEB) to complete the GFP-TonB riboregulator system.

We constructed three different GFP-TonB plasmids [RR12(11)GLT, RR12(F1)GLT, and RR12(pT1)GLT], each with different crRNA promoters. These riboregulator systems are illustrated in Fig. 2*A*, along with a depiction of GFP-TonB localization in the inner membrane. In all three plasmids, $P_{LtetO\text{-}1}$, a modified version of the native λ-phage PL promoter containing two TetR operator sites (10), regulated transcription of the taRNA. RR12(11)GLT used $P_{LtetO\text{-}1}$ as the crRNA promoter; thus GFP-TonB transcription and translation were induced by the addition of aTc. RR12(F1)GLT and RR12(pT1)GLT used P_{LfurO} (5) and pTonB (the natural TonB promoter) (18), respectively, as the crRNA promoter. P_{LfurO} is a version of the λ-phage PL promoter containing two Fur operator sites (5), and pTonB contains three Fur operator sites (18). To induce GFP-TonB expression for these plasmids, we added aTc and 2,2′-dipyridyl, an iron chelator. GFP fusion expression experiments were performed in MG1655Pro and MG1655ProΔ*tonB E. coli*.

For the toxin expression experiments, we constructed a CcdB riboregulator plasmid [RR12(14)CcdB]. This riboregulator system is illustrated in Fig. 3*A*, along with a depiction of CcdB inducing double-stranded breaks in DNA by inhibiting DNA gyrase. $P_{LtetO\text{-}1}$ drove crRNA expression, and the native, arabinose-inducible P_{BAD} promoter regulated taRNA expression. Toxin expression experiments were performed in MG1655 and MG1063 *E. coli*, which both lack the *tetR* gene (8, 9). Thus without the TetR repressor, transcription from $P_{LtetO\text{-}1}$ was constitutive. As a control for the phenotypic analyses presented in *SI Text*, we constructed a LacZ riboregulator plasmid by simply swapping in the *lacZ* gene for *ccdB*.

For the network manipulation experiments, we constructed a LexA3 riboregulator plasmid [RR12(12)LexA3]. This riboregulator system is illustrated in Fig. 4*A*, along with a depiction of LexA3 repressing a SOS gene. $P_{LtetO\text{-}1}$ drove crRNA expression, and IPTG-inducible $P_{LlacO\text{-}1}$ (10) regulated taRNA expression. $P_{LlacO\text{-}1}$ is based on the λ-phage PL promoter and contains two LacR operator sites (10). LexA3 induction experiments were performed in MG1655Pro *E. coli*.

For the orthogonal riboregulation experiments, we constructed a single plasmid [ORR(λR-R_Z+λS)] that contained two different riboregulator systems. These riboregulator systems are illustrated in Fig. 5*A*, along with a depiction of cell lysis induced by λ-phage proteins. To begin, we built the two different riboregulator variants [RR12(12)λS and RR10(14)λR-R_Z] separately. We cloned the gene *λS* into riboregulator variant crR12-taR12 and the *λR-R_Z* genes into variant crR10-taR10 (13). In both setups, $P_{LtetO\text{-}1}$ drove crRNA expression. $P_{LlacO\text{-}1}$ regulated taRNA expression in the λS riboregulator, and P_{BAD} was the taRNA promoter in the λR-R_Z riboregulator. To merge the riboregulator variants into one plasmid, we PCR amplified the entire λS riboregulator system minus the origin and resistance marker, and simultaneously added SacI restriction endonuclease recognition sites to both ends of the fragment. Finally, we inserted this fragment into the SacI recognition site of the λR-R_Z riboregulator plasmid. Clones were selected in which the transcription of λS and λR-R_Z proceeded in opposite directions. Orthogonal riboregulation experiments were performed in MG1655Pro *E. coli*.

PCR amplification was performed using the PTC-200 PCR machine (Bio-Rad) with the Phusion High-Fidelity DNA polymerase (NEB). Oligonucleotide primers were purchased from Integrated DNA Technologies. The DNA sequences for *tonB* and the natural *tonB* promoter were obtained from the MG1655 strain (8). The $P_{LtetO\text{-}1}$ and P_{BAD} sequences were obtained from our original riboregulator system (13). The P_{LfurO} sequence was obtained from the previously designed intracellular iron reporter (5). The gfp^+ sequence was obtained from the pXG-10 plasmid (19). The *ccdB* sequence was obtained from the XL10 strain. The $P_{LlacO\text{-}1}$ sequence was obtained from the pZE12G plasmid (10). The *lexA3* sequence was obtained from DM49 (F–, *lexA3*, *thr-l*, *leu-6*, *proA2*, *his-4*, *thi-1*, *argE3*, *lacY1*, *galK2*, *ara-14*, *xyl-5*, *mtl-1*, *tsx-33*, *strA31*, *sup-37*, *λ*–) (20). The *λR-R_Z* and *λS* sequences were obtained from K12 EMG2 (F+, Yale CGSC no. 4401) (21).

Microscopy (protein tracking). Cells containing a GFP-TonB fusion riboregulator plasmid were grown overnight and then diluted 1:100 in 3 mL selective LB (+30 μg/mL kanamycin). The appropriate cultures were induced at OD_{600} of 0.3–0.5. For the full induction condition in the RR12(11)GLT experiments, 100 ng/mL aTc was added to MG1655Pro and MG1655ProΔ*tonB* cells. For the 0- and 500-μM chelator conditions in the RR12(F1)GLT and RR12(pT1)GLT experiments, 100 ng/mL aTc + 0 μM 2,2′-dipyridyl and 100 ng/mL aTc + 500 μM 2,2′-dipyridyl, respectively, were added to MG1655Pro cells. At 90 min postinduction, 0.5 μL of cells was removed for fluorescent imaging at 1500× magnification using a Nikon Eclipse Ti microscope with a 100× objective, outfitted with a CoolSnap HQ^2 CCD camera (Photometrics), operated with NIS-Elements Advanced Research 3.0 software. The Nikon Intensilight C-HGFIE provided fluorescent light.

RNA microarray preparation (toxin expression). MG1655 and MG1063 cells containing RR12(14)CcdB were grown overnight and then diluted 1:1,000 in 50 mL selective LB (+30 μg/mL kanamycin) for collection of total RNA. All cultures were induced with 0.25% arabinose at OD_{600} of 0.2–0.4. Samples for transcriptome analysis were taken immediately before induction (time 0) and then at 30, 60, and 90 min postinduction. Experiments were run in duplicate. Total RNA was obtained using the RNeasy Protect Bacteria Mini Kit (Qiagen) according to manufacturer's instructions. Briefly, RNA Protect (Qiagen) was added to culture samples, which were then pelleted by centrifugation at 3000 × *g* for 15 min and stored overnight at −80 °C. Total RNA was then extracted using the RNeasy kit, and samples were DNase treated using DNA-free

(Ambion). Sample concentration was estimated using the ND-1000 spectrophotometer (NanoDrop).

cDNA was prepared from 10 μg total RNA through random primed reverse transcription, using SuperScript II (Invitrogen). The RNA was digested with the addition of 1 M NaOH and incubated at 65 °C for 30 min. The mixture was neutralized with the addition of 1 M HCl. The cDNA was purified using a QIAquick PCR purification column (Qiagen), following the manufacturer's protocol. The cDNA was fragmented to a size range of 50–200 bases with DNase I (0.6 units/g cDNA) at 37 °C for 10 min followed by inactivation of the enzyme at 98 °C for 10 min. Subsequently, the fragmented cDNA was biotin labeled using an Enzo BioArray Terminal Labeling Kit with Biotin-ddUTP (Enzo Scientific). Fragmented, biotinylated cDNA was hybridized to Affymetrix *E. coli* Antisense Genome arrays for 16 h at 45 °C and 60 rpm.

Following hybridization, arrays were washed and stained according to the standard Antibody Amplification for Prokaryotic Targets protocol (Affymetrix). The protocol consisted of a wash with nonstringent buffer, followed by a wash with stringent buffer, a stain with Strepavidin, a wash with nonstringent buffer, a stain with biotinylated anti-Strepavidin antibody, a stain with Strepavidin–Phycoerythrin, and a final wash with nonstringent buffer. The stained GeneChip arrays were scanned at 532 nm using an Affymetrix GeneChip Scanner 3000. The scanned images were scaled and quantified using GCOS v1.2 software.

RNA microarray analysis (toxin expression). The resulting *.CEL files were RMA normalized (22) and then combined with *.CEL files from microarrays comprising the M3D compendium (http://m3d.bu.edu), for a total of 505 RMA-normalized *E. coli* expression arrays. For a more robust analysis, we converted the expression values for each individual gene, at each time point (0, 30, 60, and 90 min postinduction), into estimated *z*-scores on the basis of the observed expression distribution for each gene across all experiments in the M3D compendium (23). To do so, we subtracted the mean normalized expression for each gene from its respective normalized expression for each individual experiment and then divided by the respective SD of each gene across all experiments.

To determine statistically significant changes in gene expression due to CcdB expression, we subtracted the expression *z*-score of each gene in our LacZ control dataset from the corresponding *z*-score in our CcdB dataset; again this was done for each experimental timepoint; e.g., the *z*-score of *recA* expression from our LacZ sample at 30 min was subtracted from the *recA* *z*-score from our CcdB sample at 30 min. The procedure allowed us to determine the difference in expression between a control set and a CcdB-treated dataset, subtracting out the metabolic effects of arabinose application, in terms of units of SD. A gene was considered to have significantly changed expression when its *z*-score difference was >1.5 units of SD, with the sign determining over- and underexpression.

We found the SD interval to be a robust representation of the difference of expression for all genes, including genes that may be biased due to the general and/or specific effects of the conditions reflected in the compendium; for example, several perturbations characterized by the compendium have induced increased expression of *lexA* following DNA damage response induction. More importantly, this measure was designed to be independent of a gene's dynamic range and sensitive to the statistical significance of a change of expression between the CcdB+ samples and the LacZ+ control. Thus, we were allowed to eliminate genes that change similarly over time in both expression sets and to focus on genes that change expression levels specifically as a function CcdB poisoning, using a robust statistical measure as our thresholding parameter. In this regard, it was preferable to the more usual log-ratio metric, which forces the choice of an arbitrary significance threshold independent of a gene's dynamic range.

We next used the transcription factor regulatory information contained in RegulonDB, together with a transcriptional regulatory network assembled by the CLR algorithm, to identify enriched transcription factors (23, 24). This was done in a two-step process. First, for each gene in the set of significantly changed genes, we determined its transcription factor in RegulonDB 5.0 (24). Second, starting with the most-represented regulator, we removed every gene regulated by a given transcription factor from the set of significantly changed genes, until no genes remained or until none of the remaining genes had a known transcription factor. We used the resultant set of transcription factors as an approximation of the differentially expressed transcriptional program following CcdB poisoning and determined statistical enrichment of the individual regulons of transcription factors at every time point. To this end, we restricted the list of differentially expressed genes, constructed as described above, to only those genes whose regulation was described in RegulonDB and a recently published set of regulatory connections (23). For each transcription factor database, we calculated the likelihood of finding the given number of its targets in this reduced query set using hypergeometric distribution, under the assumption that the regulon of each transcription factor was correctly and completely described by RegulonDB and the regulatory network.

To further focus our gene expression profiling, we performed functional enrichment using GO classification terms (25, 26) and the GO::TermFinder program (27). This functional enrichment was performed under the hypergeometric model of random occurrence. The purpose of this analysis method was to track temporal changes in biochemical pathways on the basis of our list of significantly changed genes.

Growth analysis and microscopy (toxin expression). Initially, we compared growth of CcdB− (uninduced cultures containing the CcdB riboregulator), CcdB+ (induced cultures containing the CcdB riboregulator), and LacZ+ (induced cultures containing the LacZ riboregulator). For these experiments, cells were grown overnight and then diluted 1:1,000 in 50 mL selective LB (+30 μg/mL kanamycin) for collection of OD_{600} and survival analysis samples. The appropriate cultures were induced with 0.25% arabinose at OD_{600} of 0.2–0.4. Light microscopy observations were taken using a Nikon Eclipse 80i microscope with a 20× objective (200× magnification), outfitted with a CoolSnap HQ CCD camera (Roper Scientific), operated with IPLab software (Scanalytics). See below for details on CFU/mL measurements.

Growth analysis (network manipulation). MG1655Pro cells containing RR12(12)LexA3 were grown overnight and then diluted 1:100 in 3 mL LB (+30 μg/mL kanamycin). The appropriate cultures were treated with 50 ng/mL norfloxacin and induced at OD_{600} between 0.3 and 0.4. The used set of inducer concentrations was determined empirically by testing a large range of concentrations. Measurements were taken with the following inducer concentrations: no inducers, 16 ng/mL aTc + 1 mM IPTG (low crRNA, high taRNA), 30 ng/mL aTc + 0.01 mM IPTG (high crRNA, low taRNA), and 30 ng/mL aTc + 1 mM IPTG (full LexA3 expression).

To measure the effect of LexA3 expression on survival, we performed a cell viability assay to measure CFU/mL. Collected samples were washed twice with filtered 1× PBS, pH 7.2 (Fisher), and then serially diluted in 1× PBS over a 6-log range. Ten microliters of each dilution were plated onto a square Petri dish (Fisher), containing 20 μL LB-Agar (Fisher), and the dish was incubated at 37 °C overnight. Only dilutions that yielded between 50 and 150 colonies were counted, and CFU/mL values were calculated using the formula ([(no. colonies) × (dilution factor)]/0.01 mL). Survival values were calculated using the formula (CFU/mL treated)/(CFU/mL untreated).

cDNA preparation (network manipulation). MG1655Pro cells containing RR12(12)LexA3 were grown overnight and then diluted 1:100 in 110 mL selective LB (+30 μg/mL kanamycin) for collection of total RNA. At OD_{600} of 0.3–0.4, four samples were started with 25 mL exponential-phase culture, and the appropriate cultures were treated with 50 ng/mL norfloxacin and induced. Measurements were taken for the genes *recA*, *recN*, *sulA*, and *umuC*, with the following inducer concentrations: no inducers, 30 ng/mL aTc + 0.01 mM IPTG (low LexA3 expression), and 30 ng/mL aTc + 1 mM IPTG (full LexA3 expression). Samples for qPCR analysis were taken immediately before treatment (time 0) and then at 30 and 90 min posttreatment. Total RNA was obtained, extracted, and purified as described above. cDNA was prepared from 5 μg total RNA through random-primed reverse transcription using SuperScript III (Invitrogen) and purified with RNase H (Ambion) treatment.

qPCR protocol and analysis (network manipulation). We performed quantitative PCR using the Roche LightCycler 480. Using the LightCycler 480 SYBR Green I Master hot-start reaction mix (Roche) and following the manufacturer's instructions, we added the following reagents to a LightCycler 480 Multiwell Plate 96: (*i*) 50 ng cDNA template, (*ii*) SYBR Green 1, (*iii*) 5 μM forward and reverse qPCR primers, and (*iv*) PCR grade water. We sealed the plate with sealing foil and spun down the plate at 3,000 rpm for 2 min before starting the qPCR reaction.

The qPCR program consisted of the following steps: preincubation, 45 amplification cycles, meting curve analysis, and a final cooling phase. Preincubation was run at 95 °C for 15 min. During amplification, the denaturation phase was run at 95 °C for 10 s, the annealing phase was run at 53 °C for 10 s, and the extension phase was run at 72 °C for 10 s. Melting curve analysis was run at 95 °C for 5 s, followed by 65 °C for 1 min, and finally at 95 °C until all DNA species had melted (continuously taking five acquisitions per second). The cooling phase was run at 40 °C for 30 s.

When analyzing the qPCR data, we averaged the mean *lplT* and *rrsH* crossing point (C_P) values, determined with the second derivative maximum method (Roche Lightcycler 480 Instrument Operator's Manual, Software Version 1.5), to arrive at a single reference C_P value. We calculated the target-reference ratios (equal to the relative mRNA concentrations) by using the following formula: $2^{\text{Target } Cp}/2^{\text{Reference } Cp}$ (Roche Lightcycler 480 Instrument Operator's Manual, Software Version 1.5). This formula assumes the PCR efficiencies = 1 and the amount of starting material in the reference and target reactions was equal. To determine the fold changes in relative mRNA concentrations for each experimental time point (Fig. 4*C*), we normalized the data with the relative concentration for the corresponding untreated (no drug or inducers) sample; e.g., the *recA* target-reference ratio value for the high LexA3 expression sample at 30 min posttreatment was divided by the *recA* target-reference ratio value for the untreated sample at 30 min posttreatment. To determine the raw relative mRNA concentrations plotted in Fig. S4, we scaled the raw target-reference ratios by 5.25×10^5, the smallest value obtained in any trial divided by 10.

Growth analysis (orthogonal riboregulation). MG1655Pro cells containing ORR(λR-R_Z+λS) were grown overnight and then diluted 1:100 in 10 mL selective LB (+30 μg/mL kanamycin) for collection of OD_{600} samples. We added 0.2% glucose (Fisher) at inoculation to the appropriate cultures. Optical density measurements were taken at 600 nm using a SPECTRAFluor Plus (Tecan). At OD_{600} between 0.7 and 0.9, the appropriate cultures were induced (Fig. 5*A*). We determined the used set of inducer concentrations empirically by testing a large range of concentrations. Measurements were taken at 0, 30, 50, and 70 min postinduction, using the following inducer concentrations: no inducers, 30 ng/mL aTc + 1 mM IPTG + 0.2% glucose (λS only), 30 ng/mL aTc + 0.01% arabinose (λR-R_Z only), and 30 ng/mL aTc + 1 mM IPTG + 0.01% arabinose (λS and λR-R_Z).

To simplify the process of simultaneously measuring a range of concentrations for each inducer, cells were grown overnight and then only a single culture was diluted 1:100 in 10 mL selective LB (+30 μg/mL kanamycin). At an OD_{600} of 0.7–0.9, we transferred 300-μL aliquots from this culture to a clear, flat bottom 96-well plate (Fisher). We tested 30 samples (three replicates of 10 different inducer concentration combinations). One sample was an untreated control. To the other 9 samples we added 30 ng/mL aTc plus different combinations of IPTG and arabinose. From high to low induction, the IPTG doses inducing λS expression were 0.1, 0.03, and 0.006 mM, and the arabinose doses inducing λR-R_Z expression were 0.01, 0.002, and 0.0003%. We incubated the 96-well plate with shaking at 900 rpm and measured OD_{600} simultaneously for all 30 samples at 20-min intervals for up to 2 h after induction. All three replicates were averaged to determine a single experimental value for each sample, and the experiment was repeated three times to calculate the triplicate mean across experiments. The full dataset is presented in Fig. S6, and a subset of the data is presented in Fig. 5 *D* and *E*.

Lysis confirmation (orthogonal riboregulation). To verify that cell lysis was responsible for the observed decreases in OD_{600}, we recorded a movie of a culture in which both λ-phage lysis proteins were fully induced (Fig. 5*B*). We induced the culture at OD_{600} of 0.3–0.4 with 30 ng/mL aTc + 1 mM IPTG + 0.01% arabinose, and a 2-μL sample was removed for observation at 45 min postinduction. To record the movie, we used a Nikon Eclipse 80i microscope with a 40× objective (400× magnification), outfitted with a CoolSnap HQ CCD camera (Roper Scientific), operated with NIS-Elements Advanced Research 3.0 software. The movie can be viewed in its entirety as Movie S1.

1. Jensen RB, Grohmann E, Schwab H, Díaz-Orejas R, Gerdes K (1995) Comparison of ccd of F, parDE of RP4, and parD of R1 using a novel conditional replication control system of plasmid R1. *Mol Microbiol* 17:211–220.
2. Jaffé A, Ogura T, Hiraga S (1985) Effects of the ccd function of the F plasmid on bacterial growth. *J Bacteriol* 163:841–849.
3. Gottesman S (1996) Proteases and their targets in Escherichia coli. *Annu Rev Genet* 30: 465–506.
4. Couturier M, Bahassi el-M, Van Melderen L (1998) Bacterial death by DNA gyrase poisoning. *Trends Microbiol* 6:269–275.
5. Dwyer DJ, Kohanski MA, Hayete B, Collins JJ (2007) Gyrase inhibitors induce an oxidative damage cellular death pathway in Escherichia coli. *Mol Syst Biol* 3:91.
6. Miyada CG, Stoltzfus L, Wilcox G (1984) Regulation of the araC gene of Escherichia coli: Catabolite repression, autoregulation, and effect on araBAD expression. *Proc Natl Acad Sci USA* 81:4120–4124.
7. Garrett JM, Young R (1982) Lethal action of bacteriophage lambda S gene. *J Virol* 44: 886–892.
8. Bachmann B (1996) Derivations and genotypes of some mutant derivatives of *Escherichia coli* K-12. Escherichia coli *and* Salmonella typhimurium: *Cellular and Molecular Biology*, eds Neidhardt F, et al. (American Society for Microbiology, Washington, DC), 2d Ed, pp 2460–2488.
9. Guyer MS (1978) The gamma delta sequence of F is an insertion sequence. *J Mol Biol* 126:347–365.
10. Lutz R, Bujard H (1997) Independent and tight regulation of transcriptional units in Escherichia coli via the LacR/O, the TetR/O and AraC/I1-I2 regulatory elements. *Nucleic Acids Res* 25:1203–1210.
11. Baba T, et al. (2006) Construction of Escherichia coli K-12 in-frame, single-gene knockout mutants: The Keio collection. *Mol Syst Biol* 2:2006–0008.
12. Datsenko KA, Wanner BL (2000) One-step inactivation of chromosomal genes in Escherichia coli K-12 using PCR products. *Proc Natl Acad Sci USA* 97:6640–6645.
13. Isaacs FJ, et al. (2004) Engineered riboregulators enable post-transcriptional control of gene expression. *Nat Biotechnol* 22:841–847.
14. Sambrook J, Fritsch EF, Maniatis T (1989) *Molecular Cloning: A Laboratory Manual* (Cold Spring Harbor Lab Press, Cold Spring Harbor, NY).
15. Kaserer WA, et al. (2008) Insight from TonB hybrid proteins into the mechanism of iron transport through the outer membrane. *J Bacteriol* 190:4001–4016.
16. Arai R, Ueda H, Kitayama A, Kamiya N, Nagamune T (2001) Design of the linkers which effectively separate domains of a bifunctional fusion protein. *Protein Eng* 14: 529–532.
17. Scholz O, Thiel A, Hillen W, Niederweis M (2000) Quantitative analysis of gene expression with an improved green fluorescent protein. *Eur J Biochem* 267:1565–1570.
18. Postle K (1990) Aerobic regulation of the Escherichia coli tonB gene by changes in iron availability and the fur locus. *J Bacteriol* 172:2287–2293.
19. Urban JH, Vogel J (2007) Translational control and target recognition by Escherichia coli small RNAs in vivo. *Nucleic Acids Res* 35:1018–1037.
20. Mount DW, Low KB, Edmiston SJ (1972) Dominant mutations (lex) in Escherichia coli K-12 which affect radiation sensitivity and frequency of ultraviolet lght-induced mutations. *J Bacteriol* 112:886–893.
21. Clowes RC, Hayes W (1968) *Experiments in Microbial Genetics* (Blackwell, Oxford).
22. Irizarry RA, et al. (2003) Exploration, normalization, and summaries of high density oligonucleotide array probe level data. *Biostatistics* 4:249–264.

23. Faith JJ, et al. (2007) Large-scale mapping and validation of Escherichia coli transcriptional regulation from a compendium of expression profiles. *PLoS Biol* 5:e8.
24. Salgado H, et al. (2006) RegulonDB (version 5.0): Escherichia coli K-12 transcriptional regulatory network, operon organization, and growth conditions. *Nucleic Acids Res* 34 (Database issue):D394–D397.
25. Ashburner M, et al.; The Gene Ontology Consortium (2000) Gene ontology: Tool for the unification of biology. *Nat Genet* 25:25–29.
26. Camon E, et al. (2004) The Gene Ontology Annotation (GOA) Database: Sharing knowledge in Uniprot with Gene Ontology. *Nucleic Acids Res* 32 (Database issue): D262–D266.
27. Boyle EI, et al. (2004) GO:TermFinder—open source software for accessing Gene Ontology information and finding significantly enriched Gene Ontology terms associated with a list of genes. *Bioinformatics* 20:3710–3715.

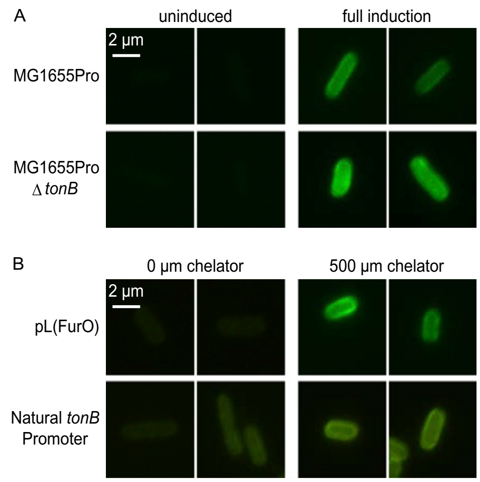

Fig. S1. Fluorescent imaging of GFP-TonB. (*A*) Representative fluorescent micrographs comparing no induction to full induction (+100 ng/mL aTc) of the fusion protein in MG1655Pro and MG1655ProΔ*tonB*. The $P_{LtetO\text{-}1}$ promoter regulated both crRNA and taRNA expression, and all images were taken at 90 min postinduction. (*B*) Representative fluorescent micrographs comparing MG1655Pro cultures with no iron chelator (+100 ng/mL aTc) to cultures with a high iron chelator concentration (+100 ng/mL aTc, +500 μM 2,2′-dipyridyl). P_{LfurO} regulates crRNA in the *Upper* images, and pTonB regulates crRNA in the *Lower* images. All images were taken at 90 min postinduction.

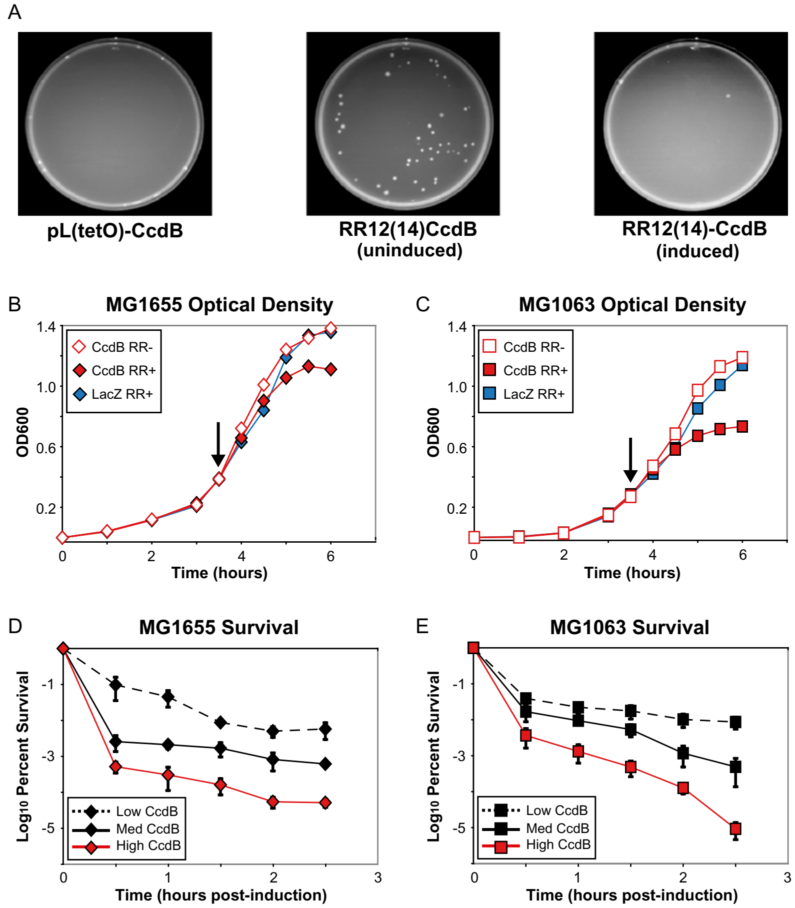

Fig. S2. Phenotypic effect of riboregulated CcdB expression in MG1655 and MG1063 *E. coli*. (*A*) Transformation of CcdB plasmids into MG1655. The CcdB riboregulator [RR12(14)CcdB] was transformed under the following conditions: uninduced and induced (+0.25% arabinose). The uninduced control plasmid [pL (tetO)-CcdB] did not contain the *cis*-repressive sequence. (*B*) Optical density of MG1655 cultures. Measurements were taken of induced LacZ control (+0.25% arabinose; blue diamonds,), uninduced CcdB (open red diamonds), and fully induced CcdB (+0.25% arabinose; solid red diamonds) cultures. Graph depicts representative measurements. (*C*) Optical density of MG1063 cultures. Measurements were taken of induced LacZ control (+0.25% arabinose; blue squares), uninduced CcdB (open red squares), and fully induced CcdB (+0.25% arabinose; solid red squares) cultures. Graph depicts representative measurements. (*D*) Log % survival of CcdB-expressing MG1655 cultures. Measurements were taken under the following conditions: +0.25% arabinose (full induction; red diamonds), +0.01% arabinose (medium induction; black diamonds, solid line), and +0.005% arabinose (low induction; black diamonds, dashed line). Graph depicts the triplicate mean ± SEM. (*E*) Log % survival of CcdB-expressing MG1063 cultures. Measurements were taken under the following conditions: +0.25% arabinose (full induction; red squares), +0.01% arabinose (medium induction; black squares, solid line), and +0.005% arabinose (low induction; black squares, dashed line). Graph depicts the triplicate mean ± SEM.

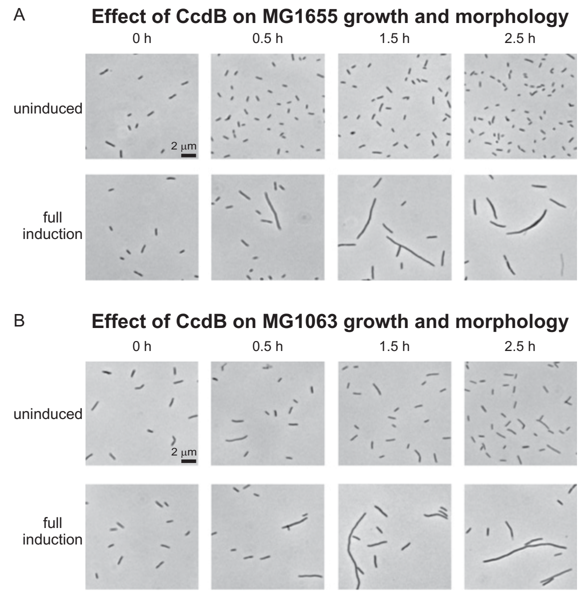

Fig. S3. Effect of riboregulated CcdB expression on morphology. Representative bright-field micrographs of CcdB riboregulator-harboring induced (+0.25% arabinose) and uninduced cultures at 0 (time 0), 0.5, 1.5, and 2.5 h postinduction are shown. (*A*) Effect of CcdB on MG1655 morphology. (*B*) Effect of CcdB on MG1063 morphology.

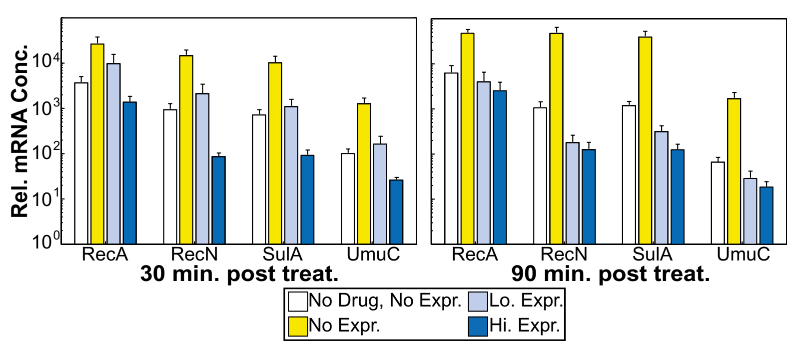

Fig. S4. Relative mRNA concentrations for selected SOS genes (*recA*, *recN*, *sulA*, *umuC*) during norfloxacin treatment and at various expression levels of LexA3. All samples, except for untreated control (white), were treated with 50 ng/mL norfloxacin. Measurements were taken at 30 (*Left*) and 90 (*Right*) min posttreatment under the following conditions: no inducers (yellow), 30 ng/mL aTc + 0.01 mM IPTG (low LexA3 expression; light blue), and 30 ng/mL aTc + 1 mM IPTG (full LexA3 expression; dark blue). Relative concentration values were calculated by normalizing with the lowest value obtained in any trial divided by 10 (5.25×10^5). Graph depicts the triplicate mean ± SEM.

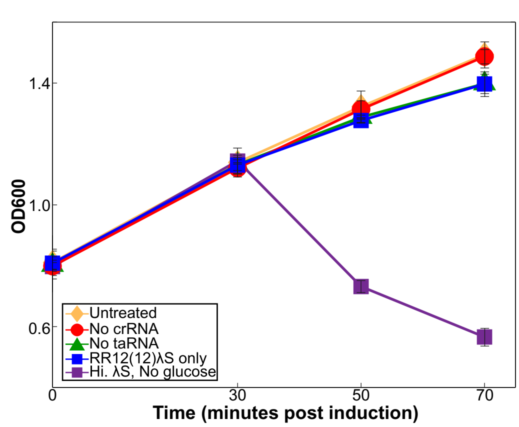

Fig. S5. Tightness of orthogonal riboregulation under various conditions. Measurements were taken under the following conditions: no inducers (untreated; orange diamonds), 1 mM IPTG + 0.01% arabinose (full induction of λS taRNA and λR-R_Z taRNA, no crRNA; red circles), 30 ng/mL aTc (full induction of λS crRNA and λR-R_Z crRNA, no taRNA; green triangles), and 30 ng/mL aTc + 1 mM IPTG (full induction of λS crRNA and taRNA, full induction of λR-R_Z crRNA only; purple squares). As a control, a strain that contains only the λS riboregulator system was fully induced (30 ng/mL aTc + 1 mM IPTG; blue squares). Graph depicts the triplicate mean ± SEM.

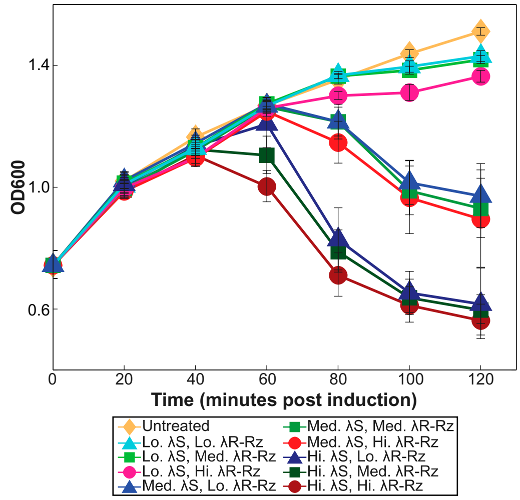

Fig. S6. Full dataset of the effect on optical density of all combinations of various λS and λR-R_Z expression levels. No inducers were added to the untreated (orange diamonds) culture. A total of 30 ng/mL aTc was added to all treated cultures to induce λS crRNA and λR-R_Z crRNA expression. High (dark colors), medium (normal colors), and low (light colors) λS expression corresponded to 0.1, 0.03, and 0.006 mM IPTG, respectively. High (circles), medium (squares), and low (triangles) λR-R_Z expression corresponded to 0.01, 0.002, and 0.0003% arabinose, respectively. Graph depicts the triplicate mean ± SEM.

Table S1. Overview of riboregulator plasmids

Plasmid name	Target gene(s)	crRNA promoter	taRNA promoter
RR12(11)GLT	*gfp-tonB* fusion	pL(tetO)	pL(tetO)
RR12(F1)GLT	*gfp-tonB* fusion	pL(furO)	pL(tetO)
RR12(pT1)GLT	*gfp-tonB* fusion	pTonB	pL(tetO)
RR12(14)CcdB	*ccdB*	pL(tetO)	pBAD
RR12(12)LexA3	*lexA3*	pL(tetO)	pL(lacO)
RR12(12)λS	*λS*	pL(tetO)	pL(lacO)
RR10(14)λR-R_Z	*λR-R_Z*	pL(tetO)	pBAD
ORR(λR-R_Z+λS)	*λR-R_Z, λS*	pL(tetO), pL(tetO)	pBAD, pL(lacO)

Information about the riboregulation systems used in this study is shown.

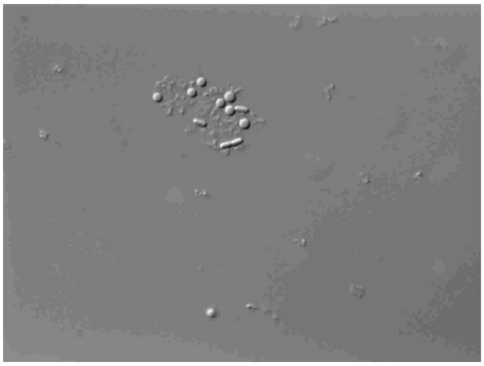

Movie S1. Confirmation of cell lysis in a fully induced culture containing ORR(λR-R_Z+λS). The movie was recorded at 45 min postinduction with 30 ng/mL aTc + 1 mM IPTG + 0.01% arabinose. Video compression was performed to minimize the file size; originally, the movie was ≈8 min long.

Movie S1

Other Supporting Information Files

Dataset S1 (XLS)
Dataset S2 (XLS)